Hindawi Publishing Corporation
International Journal of Photoenergy
Volume 2014, Article ID 834269, 9 pages
http://dx.doi.org/10.1155/2014/834269

Research Article

Equilibrium and Kinetic Aspects in the Sensitization of Monolayer Transparent TiO_2 Thin Films with Porphyrin Dyes for DSSC Applications

Rita Giovannetti, Marco Zannotti, Leila Alibabaei, and Stefano Ferraro

Chemistry Unit, School of Science and Technology, University of Camerino, Via S. Agostino 1, 62032 Camerino, Italy

Correspondence should be addressed to Rita Giovannetti; rita.giovannetti@unicam.it

Received 24 October 2013; Accepted 4 December 2013; Published 2 January 2014

Academic Editor: JiaHong Pan

Free base, Cu(II) and Zn(II) complexes of the 2,7,12,17-tetrapropionic acid of 3,8,13,18-tetramethyl-21H,23H porphyrin (CPI) in solution and bounded to transparent monolayer TiO_2 nanoparticle films were studied to determine their adsorption on TiO_2 surface, to measure the adsorption kinetics and isotherms, and to use the results obtained to optimize the preparation of DSSC photovoltaic cells. Adsorption studies were carried out on monolayer transparent TiO_2 films of a known thickness. Langmuir and Frendlich adsorption constants of CPI-dyes on TiO_2 monolayer surface have been calculated as a function of the equilibrium concentrations in the solutions. The amount of these adsorbed dyes showed the accordance with Langmuir isotherm. Kinetic data on the adsorption of dyes showed significantly better fits to pseudo-first-order model and the evaluated rate constants linearly increased with the grow of initial dye concentrations. The stoichiometry of the adsorption of CPI-dyes into TiO_2 and the influence of presence of coadsorbent (chenodeoxycholic acid) have been established. The DSSC obtained in the similar conditions showed that the best efficiency can be obtained in the absence of coadsorbent with short and established immersion times.

1. Introduction

TiO_2 is a stable, semiconductor with large band gap well known for its considerable applications in dye-sensitized solar cell (DSSC) systems [1, 2] and, for this, several preparation methods have been performed [3–6]. TiO_2 nanoparticles layer, together with the dye-sensitizer loaded on its surface, is one of the most important parts of the DSSC structure and, therefore, the optimization of these parameters can enhance the DSSC efficiency.

In the search of new dyes with high extinction coefficient and high DSSC performances, new ruthenium dyes [7], porphyrin dyes [8], and other metal-free dyes [9, 10] are synthesized.

Porphyrins are particularly interesting as photosensitizers for DSSC for the absorption in the 400–450 nm region of Soret band and in the 500–700 nm region of *Q*-bands and also for the appropriate LUMO and HOMO energy levels; this makes them promising candidates as substitutes for ruthenium dyes in DSSC applications [11].

The increase in the use of porphyrin dyes as sensitizers in DSSC has been very important to clarify the role of natural porphyrins as light harvesting in the photosynthesis; the imitation of this process has been obtained using chlorophyll derivatives as dye sensitizers for nano-TiO_2 films [12, 13], showing also the importance of free carboxylic groups for the anchoring on the TiO_2 surface [12, 14, 15]. Numerous paper reports have been published on porphyrin dyes as sensitizer for DSSC [5, 16–21].

Cu(II) and Zn(II) complexes of coproporphyrin-I (2,7,12,17-tetrapropionic acid of 3,8,13,18-tetramethyl-21H,23H porphyrin or CPI) have been synthesized in our laboratory and tested as sensitizers in DSSC [22] but mechanism and kinetic in the adsorption of these new porphyrin dyes on TiO_2 surface are not clear.

Only few studies, however, focused on kinetics and equilibrium studies on dyes sensitization [23–25]. The aim of this paper was to understand the adsorption mechanism of CPI-dyes on TiO_2, also with the use of coadsorbent, to find a suitable equilibrium isotherm and kinetic model useful to

establish the best operating conditions for the optimization of the DSSC performances. An analytical study of adsorption equilibrium and kinetic control of dyes adsorption is first presented. Successively, the optical properties of CPI-dyes TiO_2 composite thin films are investigated with the purpose of ascertaining the monolayer coverage. Finally, the results obtained are used to optimize the preparation of the photovoltaic cells.

2. Experimental

2.1. Materials. All chemicals (Sigma-Aldrich) were of analytical grade and used without further purification. All the CPI (Figure 1) solutions were prepared into anhydrous ethanol. Copper and zinc CPI complexes (CPICu and CPIZn), synthetized in our laboratory [22], are dissolved with ethanol and 10% DMSO, respectively. Solutions of chenodeoxycholic acid (4×10^{-2} M) were prepared in ethanol and in ethanol with 10% DMSO and used after dilution from 5 to 20 mM.

2.2. Transparent TiO_2 Films Fabrication. Transparent TiO2 screen-printed monolayer films used in this study were prepared, from Laboratory for Photonics and Interfaces of Ecole Polytechnique Federale of Lausanne, printing 2.7 μm thick film of 20 nm TiO_2 nanoparticles on the conducting glass electrode (fluorine doped SnO_2 (FTO)) and coating with a second layer of 5 mm thick, composed of 400 nm sized light-scattering anatase particles (CCI, Japan). TiO_2 nanoparticles and paste were prepared as described elsewhere [26]. The porosity for the 20 nm TiO_2 transparent layer, evaluated with BET measurements, was 59% (Monosorb, USA).

2.3. Optical Properties of the CPI-Dyes/TiO_2 Transparent Films. TiO_2 electrodes are sintered at 400°C, cooled to 24°C, immersed every 2 minutes in each dye solutions, washed for remove the dye molecules excess, and, at the end, dried with nitrogen. The UV-visible adsorption of dye/TiO_2 films was recorded on a Hewlett-Packard 8452A diode array spectrophotometer; the absorbance, to remove the interference, was monitored after subtracting TiO_2 film spectrum.

UV-vis absorption intensities of dyes were compared with the data of a calibration curve obtained from different reference solutions after adsorption on TiO_2 films; the content of adsorbed dyes was indicated as surface concentration of dyes (S) and was calculated as reference [23].

2.4. Device Fabrication. The sintered TiO_2 electrodes were immersed for established time in the respective dye solutions, dried by blowing nitrogen, and then assembled with a thermal platinized FTO/glass counter electrode. The working and counter electrodes, separated by a 25 mm thick hot melt ring (Surlyn, DuPont), were sealed by heating; in the internal space Z960 electrolyte [27] was added with a vacuum pump and a Surlyn sheet covered with a thin glass has been used for sealing the hole.

2.5. Photovoltaic Characterization. To characterize the solar cells, A 450 W xenon light source (Oriel, USA) was used. A Schott K113 Tempax sunlight filter (Präzisions Glas & Optik GmbH, Germany) was used to match the spectral output of the lamp in the region of 350–750 nm so as to reduce the mismatch between the simulated and true solar spectra to less than 2%. The current-voltage characteristics of the cell under these conditions were obtained by applying an external potential bias to the cell and measuring the generated photocurrent with a Keithley model 2400 digital source meter (Keithley, USA). To control the incident photon-to-current conversion efficiency (IPCE) measurement a similar data acquisition system was used. Under computer control, light from a 300 W xenon lamp (ILC Technology, USA) was focused through a Gemini-180 double monochromator (Jobin Yvon Ltd., UK) onto the photovoltaic cell under test. The devices were masked to attain an illuminated active area of 0.16 cm^2.

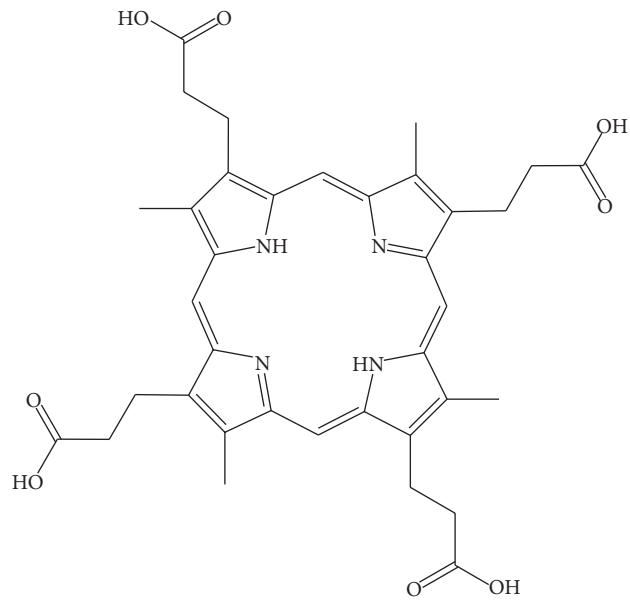

Figure 1: Molecular structure of coproporphyrin-I.

3. Results and Discussion

3.1. UV-Vis Absorption Spectra of CPI-Dyes/TiO_2 Transparent Films. Figure 2 shows the UV-vis spectra of CPI, CPIZn, and CPICu molecules adsorbed into the films and demonstrates the effective dyes adsorption into the TiO_2 films. All the spectra show the typical strong Soret band of porphyrin molecules (region 400–450 nm) and weak *Q* bands (region 500–650 nm) that are not changed with respect to solution spectra proving that, in this process, the adsorbed molecules have not modified their structural properties.

3.2. Equilibrium of CPI-Dyes Adsorption. For a good knowledge of adsorption mechanism, necessary for the optimization of the design of an adsorption system, it is important to correlate equilibrium data with theoretical and empirical equations.

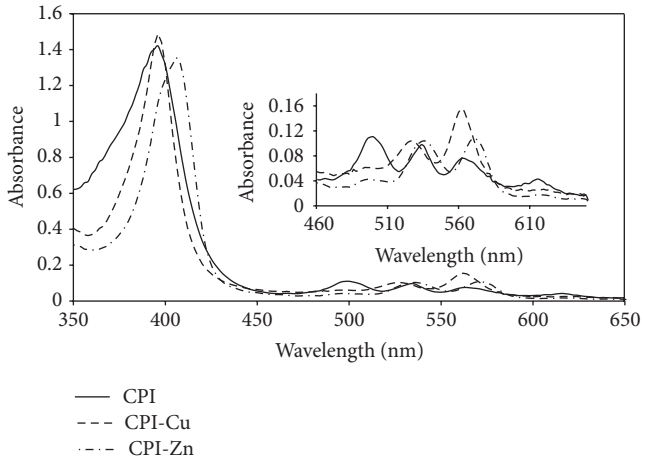

Figure 2: UV-vis spectra and in insert Q-bands magnification for CPI, CPICu, and CPIZn incorporated into the TiO_2 films.

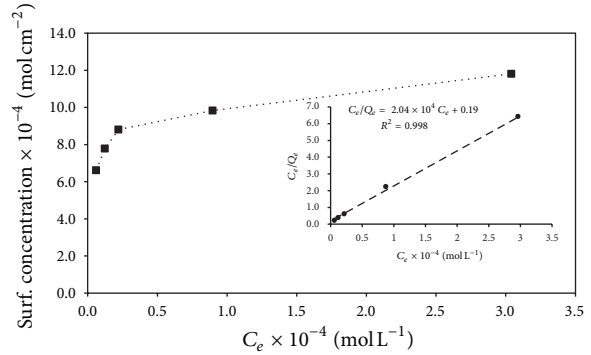

Figure 3: Grow of surface CPI concentration in the different TiO_2 films increasing CPI solution concentrations from 6.08×10^{-6} to 3.04×10^{-4} M; in insert, plot of C_e/Q_e versus C_e according to the Langmuir model.

To evaluate how the dyes concentration in the original solution influences the adsorption capacity of TiO_2 films, different concentration samples have been used. Figure 3 shows the grow of surface concentration of CPI in the different TiO_2 films increasing CPI solution concentrations. The adsorption is already high for small dye concentrations and increases to obtain a high value when the solution concentration is about 3.04×10^{-4} M; when the solutions are more concentrated, dye saturation of the film occurs. Similar behaviour has been obtained for Cu and Zn CPI-dyes.

To establish as the dye concentration influence the adsorption process, the equilibrium data has been analyzed by Freundlich (1) and Langmuir (2) isotherms [28, 29]:

$$Q_e = K_F C_e^{\,1/n} \tag{1}$$

$$Q_e = \frac{(K_L C_e)}{(1 + a_L C_e)} \tag{2}$$

where $C_e(M)$ is the concentration of the dye solution, Q_e is the amount of dye adsorbed on TiO_2 at equilibrium, K_F is the Freundlich constant that represents the adsorption capacity, $1/n$ is the adsorption intensities, K_L and a_L are the Langmuir constants, and the ratio K_L/a_L gives the theoretical saturation capacity of the TiO_2 monolayer, Q_0. The linear forms of the two equations can be, respectively, written as follows:

$$\ln Q_e = \ln K_F + \left(\frac{1}{n}\right) \ln C_e \qquad \frac{C_e}{Q_e} = \left(\frac{1}{K_L}\right) + \left(\frac{a_L}{K_L}\right) C_e. \tag{3}$$

The linearized isotherm plots were used to calculate the adsorption isotherm constants and the results were summarized in Table 1 that shows the adsorption data fitting to the Langmuir and Freundlich isotherm models.

The correlation coefficients (R_L^2) for the Langmuir isotherm are highest in comparison to the values obtained for the Freundlich (R_F^2) isotherms, indicating that, in the studied concentration range, a Langmuir adsorption relation

Table 1: Langmuir (L) and Freundlich (F) CPI-dyes adsorption constants on TiO_2 monolayer surface.

	CPI	CPI-Zn	CPI-Cu
K_L	5.051	3.178	3.037
Q_0	4.90×10^{-5}	5.03×10^{-5}	6.50×10^{-5}
a_L	1.03×10^5	6.31×10^4	4.67×10^4
R_L^2	0.998	0.999	0.998
K_F	7.005	2.323	1.732
R_F^2	0.965	0.805	0.825

provides a good description of the CPI-dyes/TiO_2 interaction during the adsorption process. As example the plot of C_e/Q_e versus C_e is shown in insert of Figure 3 for CPI adsorption, and the other CPI-dyes show similar behaviour.

According to the Langmuir model, it may be deduced that, in this adsorption process, all dye molecules incorporated into the film have similar adsorption energy, the number of adsorption sites is limited, and the maximum adsorption corresponds to a saturated one layer of dye molecules on the adsorbent TiO_2 surface that cannot contribute to an additional incorporation of other molecules.

Interesting to note that, using CPI, when its concentration is greater than 3.04×10^{-4} M, the autoadsorption of dye occurred on TiO_2 surface, for probable dye aggregation. In fact, poorly resolved spectrum in the Soret band has been obtained while the absorbance profile in the Q band show typical spectrum of CPI aggregates [22] as reported in Figure 4. Similar behaviour is not obtained for the other CPI-dyes because, for the influence of central metal ion in the complexes, the aggregation of these may occur only at highest concentration.

3.3. Kinetics of CPI-Dyes Adsorption. The absorption of CPI-dyes molecules into TiO_2 films was strictly depending on the immersion time as reported in Figure 5 that shows the spectral change in the time for CPIZn dyes adsorbed into monolayer transparent TiO_2 films and the evolution in the

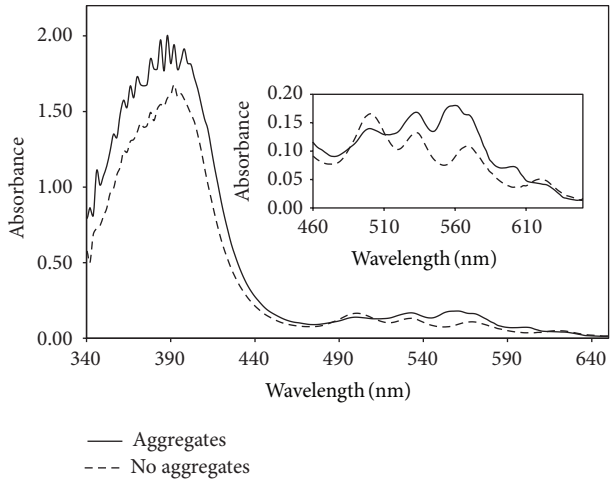

Figure 4: Absorbance profiles in the Q band: comparison between UV-vis spectra of CPI, aggregates (3.04×10^{-4} M) and no aggregates (8.96×10^{-5} M), adsorbed into TiO_2 films.

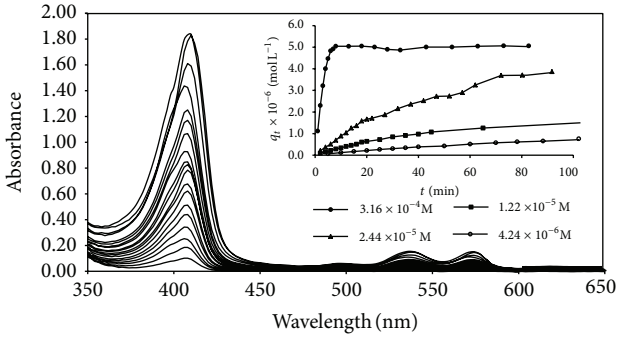

Figure 5: Spectral change in the time of CPIZn adsorbed on TiO_2 surface after immersion into CPIZn solution of 2.44×10^{-5} M; in insert evolution in the time of CPIZn surface concentrations q_t for different initial solution concentrations.

time of the surface concentrations of dyes q_t at different solution concentrations of dyes.

The curves obtained at higher dyes concentration show two zones: in the first, the amount of adsorbed molecules grows rapidly while in the second a slowdown of the process occurs because the saturation approaches; all the results showed that the absorption rates depended on initial dye concentrations.

For a correct interpretation of the absorption kinetics, the experimental points were compared with different adsorption kinetic models and the best fit has been observed with a pseudo-first-order model that is a procedure frequently used for the adsorption of a solute from solution [30] and can be expressed by:

$$q_t = q_e \left[1 - \exp\left(-k_1 t\right)\right] \quad (4)$$

where q_t is the amount of dye adsorbed at time t, q_e is equilibrium solid phase concentration, and k_1 is first-order

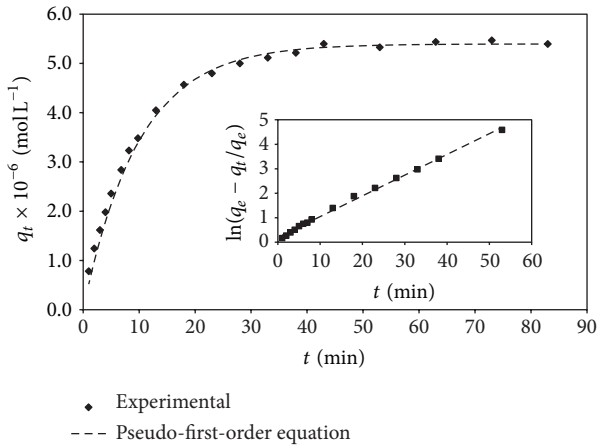

Figure 6: Comparison between measured and modelled time profiles for the adsorption of 8.96×10^{-5} M of CPI.

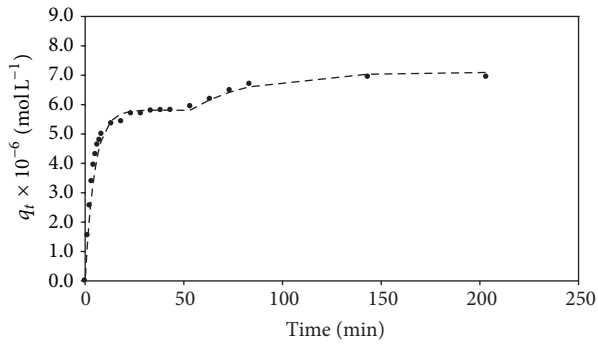

Figure 7: Evolution in the time of the CPI surface concentration Q_t with CPI concentration of 3.04×10^{-4} M.

rate constant for adsorption. The linear form is given as follows:

$$\ln\left[\frac{(q_e - q_t)}{q_e}\right] = -k_1 t. \quad (5)$$

Plotting the first term of (5) versus t, good straight lines are obtained and the values of k_1 can be deduced (Tables 2, 3, and 4). In the insert of Figure 6 a comparison of calculated and measured results for 8.96×10^{-5} M of CPI-dyes, over the entire range of time studied, is reported as an example, showing a good fit to the model; the results indicate therefore that the pseudo-first-order equation provides the best correlation for the these adsorption processes.

However, only for CPI, at concentration of 3.04×10^{-4} M, the adsorption took place in two stages (Figure 7) that followed first-order kinetics with respect to CPI concentrations: in the first stage quickly adsorption of CPI occurred while in the slower second step an autoadsorption of CPI was observed.

In Table 2 are reported the values of respective kinetic constants that demonstrate that the monolayer adsorption is about six time faster with respect to layer on layer CPI adsorption. This result can be explained by the adsorption/aggregation competition between CPI molecules and

Table 2: Kinetic constants for adsorption of different CPI concentrations on TiO_2.

CPI mol L^{-1}	k_1 l mol^{-1} min^{-1}
6.08×10^{-6}	3.54×10^{-3}
1.23×10^{-5}	1.02×10^{-2}
2.21×10^{-5}	1.34×10^{-2}
8.96×10^{-5}	1.01×10^{-1}
3.04×10^{-4}	19.31×10^{-1}*
3.04×10^{-4}	3.21×10^{-1}°
$k_1 = 1188.9\, C_{CPI} - 0.0066$	$R^2 = 0.992$

*first step kinetic; °second step kinetic.

Table 3: Kinetic constants for adsorption of different CPIZn concentrations on TiO_2.

CPIZn mol L^{-1}	k_1 l mol^{-1} min^{-1}
4.24×10^{-6}	3.41×10^{-3}
1.22×10^{-5}	1.48×10^{-2}
2.44×10^{-5}	3.73×10^{-2}
3.16×10^{-4}	64.67×10^{-2}
$k_1 = 2.08 \times 10^3\, C_{CPIZn} - 9.68 \times 10^{-3}$	$R^2 = 0.999$

their aggregate forms, which could be more significant with higher concentration of CPI solutions.

The values of the kinetic constants obtained, reported in Tables 2–4, are in accordance with those of other authors [24] and indicate that the rate of dyes adsorption linearly increases with the growing of initial solutions concentrations of dyes and also that the dependence of rate constants with the dye concentrations shows high correlation and can be expressed by linear equations.

3.4. Effect of Chenodeoxycholic Acid on the Dyes Adsorption. The effect of aggregation on the TiO_2 surface must be carefully considered and clarified for improving the cell performance of porphyrin-based DSSC [31]; the porphyrin molecules aggregation is the result of π-stacking and is a serious problem because the aggregates do not generate photocurrent [31]. The addition of a coadsorbent onto the dye solutions, during the dye-coating process, can be useful for the suppression of dye aggregation on the TiO_2 surface. Chenodeoxycholic acid (CDCA) is the most popular coadsorbent that, adsorbing on the TiO_2 surface thanks to their carboxyl and hydroxyl groups, restricting dye aggregation in DSSC assembly [18, 32].

For evaluating the effect of CDCA concentrations on the adsorption of CPI-dyes on TiO_2 surfaces, solutions of dyes with different CDCA concentrations have been used. In Figure 8 are reported, as example, the adsorption kinetics for CPI varying the CDCA concentrations, which clearly demonstrate that the adsorption of dyes decreased with an competitive effect on the adsorption that depended on CDCA concentrations. Also the kinetics of these process changed

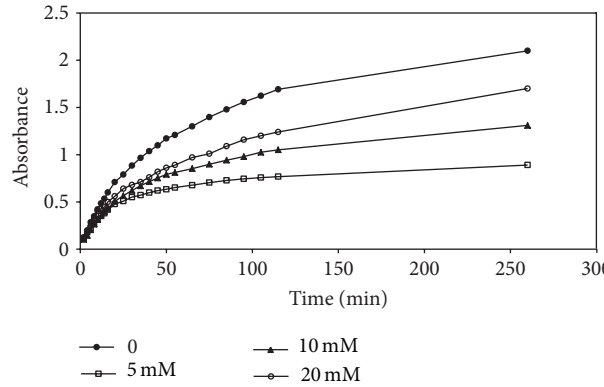

Figure 8: Effect of CDCA concentration from 0 to 20 mM on the adsorption of CPI 2.21×10^{-5} M.

Table 4: Kinetic constants for adsorption of different CPICu concentrations on TiO_2.

CPICu mol L^{-1}	k_1 l mol^{-1} min^{-1}
3.23×10^{-6}	4.91×10^{-2}
1.50×10^{-5}	1.89×10^{-2}
3.01×10^{-5}	4.01×10^{-2}
2.47×10^{-4}	23.85×10^{-2}
$k_1 = 9.44 \times 10^2\, C_{CPICu} + 5.89 \times 10^{-3}$	$R^2 = 0.999$

Table 5: Comparison between the degree of covering, theoretical $(DC)_T$ and experimental $(DC)_E$ for different CPI-dyes.

Dyes	Concentration (M)	CDCA (mM)	$(DC)_T/(DC)_E$
CPI	3.04×10^{-4}	0	0.943
		2	0.888
		10	0.747
		20	0.393
CPI-Zn	3.04×10^{-4}	0	0.939
		2	0.908
		20	0.648
CPI-Cu	3.04×10^{-4}	0	1.011
		2	0.935
		20	0.843

confirming the competition of CDCA in the adsorption of CPI-dyes for the suppression of the adsorption of CPI-dye molecules on the TiO_2 surface.

3.5. Stoichiometry of the Adsorption Process and Photovoltaic Measurements. The evaluation of the number of CPI-dye molecules adsorbed on the TiO_2 surface permits calculating the stoichiometry of the adsorption process. The effective adsorption surface of TiO_2 monolayer has been calculated from the TiO_2 roughness [33], porosity, and exposed surface parameters. Therefore, assuming full coverage of this, it is possible to estimate the number of CPI-dye molecules which

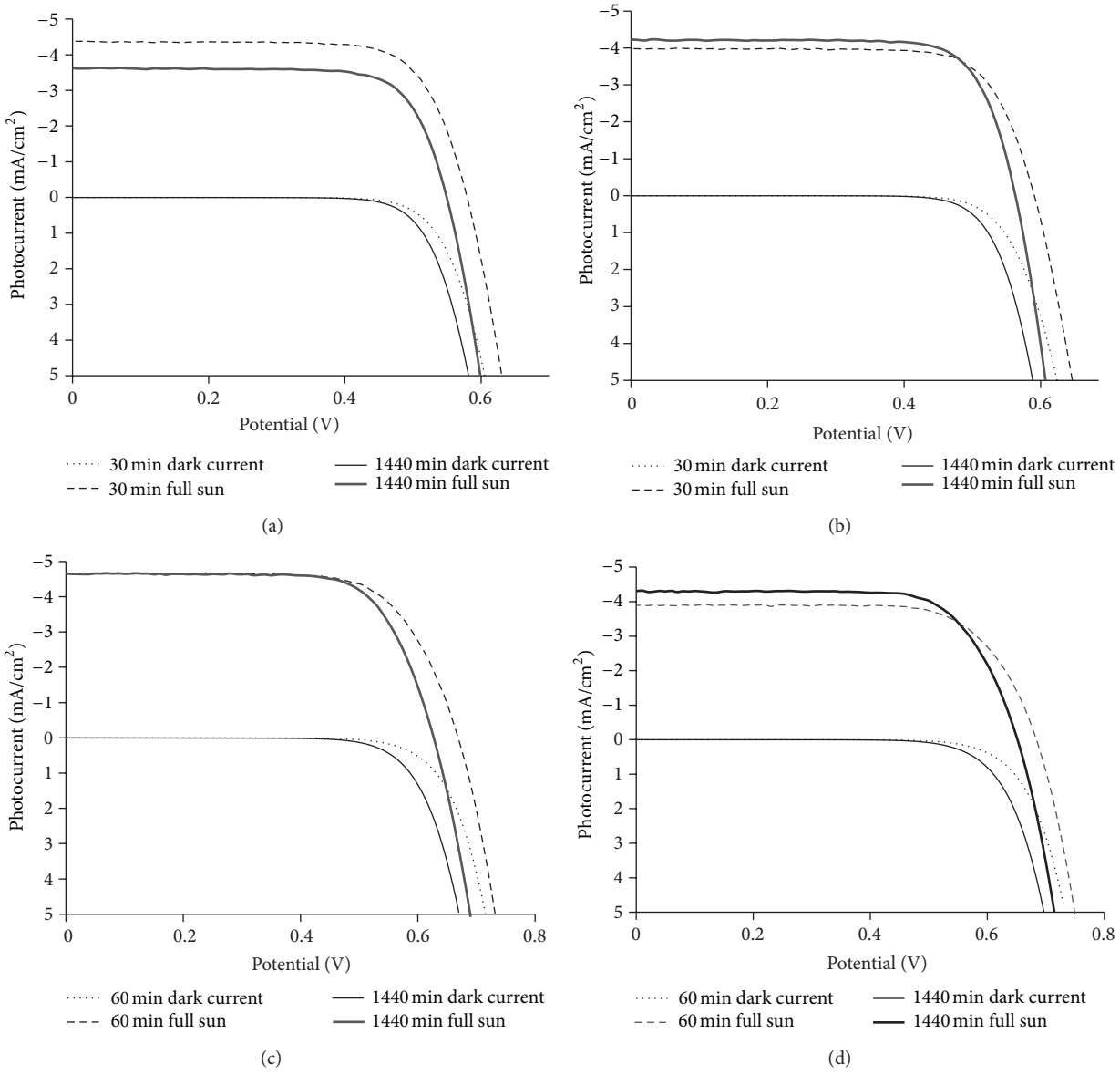

Figure 9: Photocurrent-voltage curves of dye-sensitized solar cells with different adsorption times for (a) CPIZn solution 3.04×10^{-4} M without CDCA, (b) CPIZn solution with CDCA 2 mM, (c) CPICu solution 3.04×10^{-4} M without CDCA, and (d) CPICu solution with CDCA 2 mM.

could be adsorbed. Knowing in fact the effective surface area of CPI-dye molecules that is approximately 1.31×10^{-14} cm^2, it is possible to calculate the theoretical degree of covering $(DC)_T$ that can be compared with that experimental $(DC)_E$ as reported in Table 5.

From the ratio between theoretical $(DC)_T$ and experimental $(DC)_E$ values, obtained after immersion of 30 min for CPIZn and 60 min for CPI and CPICu with different CDCA concentrations, it may be deduced that the CPI-dyes form a single layer on the TiO_2 surface, in which the increase of CDCA concentration causes a competition with the dyes to the active sites on the semiconductor and consequently less dye molecules are adsorbed.

From the results obtained, since the amount of dye adsorbed on the TiO_2 film changed with time and with CDCA concentrations, it was also interesting to investigate the change of photovoltaic properties with adsorption time and coadsorbent.

Figure 9 shows the results of photocurrent-voltage curves for different experimental conditions of CPIZn and CPICu dye solutions, respectively, and the relevant photovoltaic parameters are listed in Table 6.

It is very important to consider that in the presence of CDCA 2 mM the Voc values increased but, only at long adsorption times, this is translatable in an increase in efficiency.

Table 6: Effects of adsorption time and CDCA on the short-circuit photocurrent density (Jsc) open-circuit voltage, fill factor (FF), and overall conversion efficiency (η) of dye-sensitized solar cells based on CPICu and CPIZn (0.3 mM) with 2.7 μm thick monolayer TiO_2 film and using Z960 as electrolyte under an illumination of the AM 1.5G full sunlight intensity.

	Dye	CDCA	Adsorption time (min)	Jsc (mA/cm^2)	Module U_{oc} (mV)	FF	η (%)
(a)	CPIZn	—	1440	3.62	549.12	73.54	1.48
	CPIZn	—	30	4.38	579.10	70.36	1.86
(b)	CPIZn	2 mM	1440	4.23	562.48	69.88	1.80
	CPIZn	2 mM	30	3.98	590.31	70.96	1.77
(c)	CPICu	—	1440	4.66	626.64	71.85	2.10
	CPICu	—	60	4.65	668.20	70.36	2.20
(d)	CPICu	2 mM	1440	4.70	650.19	69.88	2.14
	CPICu	2 mM	60	3.89	686.50	70.94	1.89

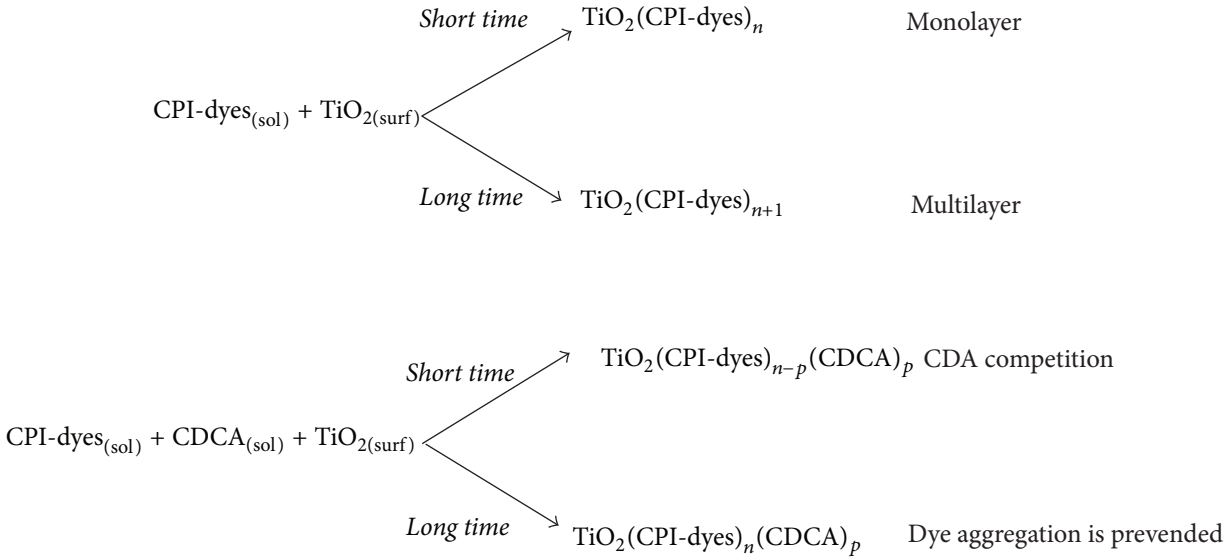

Figure 10

In fact, as it can be seen in Table 6, for the CPIZn dye, in the presence of CDCA 2 mM and with the adsorption time of 1440 min, the efficiency is greater than that in absence of CDCA; on the contrary when the adsorption time is of 30 min, in the presence of CDCA, the efficiency is lower with respect to that without CDCA; similar results were obtained with CPICu.

However, in the absence of CDCA, monolayer coverage is expected to be formed in 30 min for CPIZn and 60 min for CPICu, while multilayer (due to dye aggregation) is expected only after these times. Because the dye aggregates have been known to be inactive for electron injection and shield the dye molecules in direct contact with TiO_2 from absorbing light, it is thus expected that, in the absence of CDCA, long adsorption time exhibits lower photocurrent in spite of higher dye loading.

The best efficiencies are obtained at 30 min adsorption from CPIZn solution and at 60 min adsorption from CPICu, in the absence of CDCA, condition in which a single layer of the dyes is obtained as verified from the stoichiometry of adsorption process (see Table 5).

So, for both CPIZn and CPICu the use of CDCA is negative for short immersion times because, thank of its competition with CPI-dyes, the dye coverage on TiO_2 surface decrease, while is positive only with long immersion times probably because it permits the evolution of adsorption process with reduction of dye aggregation on the TiO_2 surface. For these results the adsorption mechanisms of CPI-dyes in the presence and in the absence of CDCA can be explained as shown in Figure 10.

4. Conclusions

For the best manufacture of DSSC devices, optimum objectives are represented by very rapid and complete adsorption of single layer of dye on the semiconductor surface.

In this study we have described that the CPI-dyes concentration and adsorption times affected the dyes adsorption

on TiO_2 monolayer surfaces and consequently the DSSC performances.

The analytical study, with the equilibrium and kinetic data presented for adsorption of CPI-dyes onto TiO_2 monolayer surfaces, also in the presence of CDCA as coadsorbent, has allowed us to establish the best experimental conditions for the adsorption of these dyes and has demonstrated that the CPI-dyes, according to the Langmuir model and with pseudo-first-order kinetics, are adsorbed effectively on the TiO_2 monolayer without chemical changes. A systematic study of kinetic and equilibrium has been proposed demonstrating that the suppression of the dyes aggregation permits the optimization of selective adsorption of one layer of dyes molecules to stoichiometric ratios indicating a powerful strategy, which can be applied to other dyes, for improving performances in DSSC.

Conflict of Interests

The authors declare that there is no conflict of interests regarding the publication of this article.

Acknowledgments

The authors gratefully appreciate Professor Grätzel and Dr. Shaik M. Zakeeruddin of Ecole Polytechnique Federale of Lausanne, for allowing and facilitating Leila Alibabaei in assembling cells and on photovoltaic measurements. The authors also thanks Dr. Takeru Bessho for fabricated TiO_2 electrodes and Professor Vito Bartocci for fruitful discussions.

References

[1] M. Grätzel, "Photoelectrochemical cells," *Nature*, vol. 414, no. 6861, pp. 338–344, 2001.

[2] A. Hagfeldt, G. Boschloo, L. Sun, L. Kloo, and H. Pettersson, "Dye-sensitized solar cells," *Chemical Reviews*, vol. 110, no. 11, pp. 6595–6663, 2010.

[3] K.-M. Lee, V. Suryanarayanan, and K.-C. Ho, "Influences of different TiO_2 morphologies and solvents on the photovoltaic performance of dye-sensitized solar cells," *Journal of Power Sources*, vol. 188, no. 2, pp. 635–641, 2009.

[4] K. Fan, T. Peng, J. Chen, X. Zhang, and R. Li, "A simple preparation method for quasi-solid-state flexible dye-sensitized solar cells by using sea urchin-like anatase TiO_2 microspheres," *Journal of Power Sources*, vol. 222, pp. 38–44, 2013.

[5] C.-R. Ke and J.-M. Ting, "Anatase TiO_2 beads having ultra-fast electron diffusion rates for use in low temperature flexible dye-sensitized solar cells," *Journal of Power Sources*, vol. 208, pp. 316–321, 2012.

[6] X. Chen and S. S. Mao, "Titanium dioxide nanomaterials: synthesis, properties, modifications and applications," *Chemical Reviews*, vol. 107, no. 7, pp. 2891–2959, 2007.

[7] A. Sepehrifard, S. Chen, A. Stublla, P. G. Potvin, and S. Morin, "Effects of ligand LUMO levels, anchoring groups and spacers in Ru(II)-based terpyridine and dipyrazinylpyridine complexes on adsorption and photoconversion efficiency in DSSCs," *Electrochimica Acta*, vol. 87, pp. 236–244, 2013.

[8] A. Yella, H.-W. Lee, H. N. Tsao et al., "Porphyrin-sensitized solar cells with cobalt (II/III)-based redox electrolyte exceed 12 percent efficiency," *Science*, vol. 334, no. 6056, pp. 629–634, 2011.

[9] S. Ramkumar and S. Anandan, "Synthesis of bioanchored metal free organic dyes for dye sensitized solar cells," *Dyes and Pigments*, vol. 97, no. 3, pp. 397–404, 2013.

[10] R. Sirohi, D. H. Kim, S.-C. Yu, and S. H. Lee, "Novel di-anchoring dye for DSSC by bridging of two mono anchoring dye molecules: a conformational approach to reduce aggregation," *Dyes and Pigments*, vol. 92, no. 3, pp. 1132–1137, 2012.

[11] M. K. Panda, K. Ladomenou, and A. G. Coutsolelos, "Porphyrins in bio-inspired transformations: light-harvesting to solar cell," *Coordination Chemistry Reviews*, vol. 256, no. 21-22, pp. 2601–2627, 2012.

[12] W. M. Campbell, A. K. Burrell, D. L. Officer, and K. W. Jolley, "Porphyrins as light harvesters in the dye-sensitised TiO_2 solar cell," *Coordination Chemistry Reviews*, vol. 248, no. 13-14, pp. 1363–1379, 2004.

[13] R. Dabestani, A. J. Bard, A. Campion et al., "Sensitization of titanium dioxide and strontium titanate electrodes by ruthenium(II) tris(2,2′-bipyridine-4,4′-dicarboxylic acid) and zinc tetrakis(4-carboxyphenyl)porphyrin: an evaluation of sensitization efficiency for component photoelectrodes in a multipanel device," *The Journal of Physical Chemistry*, vol. 92, no. 7, pp. 1872–1878, 1988.

[14] G. K. Boschloo and A. Goossens, "Electron trapping in porphyrin-sensitized porous nanocrystalline TiO_2 electrodes," *The Journal of Physical Chemistry*, vol. 100, no. 50, pp. 19489–19494, 1996.

[15] C. C. Wamser, H.-S. Kim, and J.-K. Lee, "Solar cells with porphyrin sensitization," *Optical Materials*, vol. 21, no. 1–3, pp. 221–224, 2003.

[16] D. Daphnomili, G. D. Sharma, S. Biswas, K. R. J. Thomas, and A. G. Coutsolelos, "A new porphyrin bearing a pyridinylethynyl group as sensitizer for dye sensitized solar cells," *Journal of Photochemistry and Photobiology A*, vol. 253, pp. 88–96, 2013.

[17] T. Ma, K. Inoue, K. Yao et al., "Photoelectrochemical properties of TiO_2 electrodes sensitized by porphyrin derivatives with different numbers of carboxyl groups," *Journal of Electroanalytical Chemistry*, vol. 537, no. 1-2, pp. 31–38, 2002.

[18] Q. Wang, W. M. Campbell, E. E. Bonfantani et al., "Efficient light harvesting by using green Zn-porphyrin-sensitized nanocrystalline TiO_2 films," *The Journal of Physical Chemistry B*, vol. 109, no. 32, pp. 15397–15409, 2005.

[19] M. K. Nazeeruddin, R. Humphry-Baker, D. L. Officer, W. M. Campbell, A. K. Burrell, and M. Grätzel, "Application of metalloporphyrins in nanocrystalline dye-sensitized solar cells for conversion of sunlight into electricity," *Langmuir*, vol. 20, no. 15, pp. 6514–6517, 2004.

[20] W. M. Campbell, K. W. Jolley, P. Wagner et al., "Highly efficient porphyrin sensitizers for dye-sensitized solar cells," *The Journal of Physical Chemistry C*, vol. 111, no. 32, pp. 11760–11762, 2007.

[21] M. Gervaldo, F. Fungo, E. N. Durantini, J. J. Silber, L. Sereno, and L. Otero, "Carboxyphenyl metalloporphyrins as photosensitizers of semiconductor film electrodes. A study of the effect of different central metals," *The Journal of Physical Chemistry B*, vol. 109, no. 44, pp. 20953–20962, 2005.

[22] L. Alibabaei, M. Wang, R. Giovannetti et al., "Application of Cu(ii) and Zn(ii) coproporphyrins as sensitizers for thin film dye sensitized solar cells," *Energy and Environmental Science*, vol. 3, no. 7, pp. 956–961, 2010.

[23] P. Castillero, J. R. Sánchez-Valencia, M. Cano et al., "Active and optically transparent tetracationic porphyrin/TiO_2 composite thin films," *ACS Applied Materials and Interfaces*, vol. 2, no. 3, pp. 712–721, 2010.

[24] C.-R. Lee, H.-S. Kim, I.-H. Jang, J.-H. Im, and N.-G. Park, "Pseudo first-order adsorption kinetics of N719 dye on TiO_2 surface," *ACS Applied Materials and Interfaces*, vol. 3, no. 6, pp. 1953–1957, 2011.

[25] P. J. Holliman, B. Vaca Velasco, I. Butler, M. Wijdekop, and D. A. Worsley, "Studies of dye sensitisation kinetics and sorption isotherms of direct red 23 on titania," *International Journal of Photoenergy*, vol. 2008, Article ID 827605, 7 pages, 2008.

[26] P. Wang, S. M. Zakeeruddin, J.-E. Moser, and M. Grätzel, "A new ionic liquid electrolyte enhances the conversion efficiency of dye-sensitized solar cells," *The Journal of Physical Chemistry B*, vol. 107, no. 48, pp. 13280–13285, 2003.

[27] L. Alibabaei, J.-H. Kim, M. Wang et al., "Molecular design of metal-free D-π-A substituted sensitizers for dye-sensitized solar cells," *Energy and Environmental Science*, vol. 3, no. 11, pp. 1757–1764, 2010.

[28] M. Özacar and I. A. Şengil, "Equilibrium data and process design for adsorption of disperse dyes onto alunite," *Environmental Geology*, vol. 45, no. 6, pp. 762–768, 2004.

[29] M. Özacar, "Equilibrium and kinetic modelling of adsorption of phosphorus on calcined alunite," *Adsorption*, vol. 9, no. 2, pp. 125–132, 2003.

[30] A. Günay, E. Arslankaya, and I. Tosun, "Lead removal from aqueous solution by natural and pretreated clinoptilolite: adsorption equilibrium and kinetics," *Journal of Hazardous Materials*, vol. 146, no. 1-2, pp. 362–371, 2007.

[31] J. Rochford, D. Chu, A. Hagfeldt, and E. Galoppini, "Tetrachelate porphyrin chromophores for metal oxide semiconductor sensitization: effect of the spacer length and anchoring group position," *Journal of the American Chemical Society*, vol. 129, no. 15, pp. 4655–4665, 2007.

[32] K. Hara, Y. Dan-Oh, C. Kasada et al., "Effect of additives on the photovoltaic performance of coumarin-dye- sensitized nanocrystalline TiO_2 solar cells," *Langmuir*, vol. 20, no. 10, pp. 4205–4210, 2004.

[33] S. H. Kang, J.-Y. Kim, and Y.-E. Sung, "Role of surface state on the electron flow in modified TiO_2 film incorporating carbon powder for a dye-sensitized solar cell," *Electrochimica Acta*, vol. 52, no. 16, pp. 5242–5250, 2007.